Monthly Notices of the ROYAL ASTRONOMICAL SOCIETY

MNRAS **461,** 3165–3171 (2016) doi:10.1093/mnras/stw1468
Advance Access publication 2016 June 20

Soft γ-ray selected radio galaxies: favouring giant size discovery

L. Bassani,[1⋆] T. Venturi,[2] M. Molina,[1] A. Malizia,[1⋆] D. Dallacasa,[2,3] F. Panessa,[4] A. Bazzano[4] and P. Ubertini[4]

[1] *INAF/IASF Bologna, Via P. Gobetti 101, I-40129 Bologna, Italy*
[2] *INAF/IRA Bologna, Via P. Gobetti 101, I-40129 Bologna, Italy*
[3] *Dipartimento di Fisica e Astronomia, Universitá di Bologna, Via Ranzani 1, I-40127 Bologna, Italy*
[4] *INAF/IAPS Roma, Via Fosso del Cavaliere 100, I-00133 Rome, Italy*

Accepted 2016 June 15. Received 2016 June 15; in original form 2016 January 28

ABSTRACT

Using the recent *INTEGRAL*/IBIS and *Swift*/BAT surveys we have extracted a sample of 64 confirmed plus three candidate radio galaxies selected in the soft gamma-ray band. The sample covers all optical classes and is dominated by objects showing a Fanaroff–Riley type II radio morphology; a large fraction (70 per cent) of the sample is made of 'radiative mode' or high-excitation radio galaxies. We measured the source size on images from the NRAO VLA Sky Survey, the Faint Images of the Radio Sky at twenty-cm and the Sydney University Molonglo Sky Survey images and have compared our findings with data in the literature obtaining a good match. We surprisingly found that the soft gamma-ray selection favours the detection of large size radio galaxies: 60 per cent of objects in the sample have size greater than 0.4 Mpc while around 22 per cent reach dimension above 0.7 Mpc at which point they are classified as giant radio galaxies (GRGs), the largest and most energetic single entities in the Universe. Their fraction among soft gamma-ray selected radio galaxies is significantly larger than typically found in radio surveys, where only a few per cent of objects (1–6 per cent) are GRGs. This may partly be due to observational biases affecting radio surveys more than soft gamma-ray surveys, thus disfavouring the detection of GRGs at lower frequencies. The main reasons and/or conditions leading to the formation of these large radio structures are still unclear with many parameters such as high jet power, long activity time and surrounding environment all playing a role; the first two may be linked to the type of active galactic nucleus discussed in this work and partly explain the high fraction of GRGs found in the present sample. Our result suggests that high energy surveys may be a more efficient way than radio surveys to find these peculiar objects.

Key words: galaxies: active – gamma-rays: galaxies – radio continuum: galaxies.

1 INTRODUCTION

A small fraction of radio galaxies [around 6 per cent in the Revised Third Cambridge Catalogue of Radio Sources (3CR); Ishwara-Chandra & Saikia, 1999] exhibit extraordinary linear extents, i.e. above 0.7 Mpc (for $H_0 = 71$ km s^{-1} Mpc^{-1}, $\Omega = 0.27$, $\Omega_\Lambda = 0.73$). Defined as giant radio galaxies (GRGs), these objects represent the largest and most energetic single entities in the Universe and are of particular interest as extreme examples of radio source development and evolution; indeed they are the ideal targets to study the duty cycle of radio activity. Furthermore, it has been proposed that they can play a role in the formation of large-scale structures and can be used to probe the warm-hot intergalactic medium (Malarecki et al. 2013). In addition, GRGs are unique laboratories to study particle acceleration processes and understand cosmic magnetism (Kronberg et al. 2004).

GRGs are difficult to discover for two main reasons: (a) the low surface brightness of their extended emission requires sensitive radio telescopes to be detected and (b) they are often composed of bright knots spread over a large area which are difficult to associate to a single radio source. As a result, only around 300 GRGs are known to date (Wezgowiec, Jamrozy & Mack 2016, and references therein).

Both Fanaroff–Riley type I and type II radio galaxies (FR I and FR II, respectively; Fanaroff & Riley 1974) are represented in samples of GRGs. While FR I GRGs are associated with early-type galaxies, those with FR II morphology are hosted both in early-type galaxies and quasars. Lara et al. (2001, 2004) studied the statistical properties of a sample of GRGs selected from the NRAO VLA Sky

⋆ E-mail: bassani@iasfbo.inaf.it (LB); malizia@iasfbo.inaf.it (AM)

Survey (NVSS) and found roughly the same fraction of FR I and FR II sources, the FR IIs being at much higher redshifts mainly due to the fact that they have higher power and are edge brightened. The samples of GRGs available in the literature, mainly drawn from radio surveys such as the NVSS, the Sydney University Molonglo Sky Survey (SUMSS) and the Westerbork Northern Sky Survey (WENSS; Cotter, Rawlings & Saunders 1996; Lara et al. 2001; Machalski, Jamrozy & Zola 2001; Schoenmakers et al. 2001; Saripalli et al. 2005; Machalski & Jamrozy 2006), have been used to test models of radio galaxy evolution (e.g. Blundell, Rawlings & Willott 1999). On the basis of the assumption that spectral ages of radio galaxies are representative of their intrinsic ages (Parma et al. 1999),[1] GRGs are found to be on average old sources with measured radiative ages in excess of 10^8 yr.

Beyond the source age, the main intrinsic parameters which allow a radio galaxy to reach a linear size of the order of the Mpc during its lifetime are still unclear. The role of the external medium is difficult to evaluate, not to mention that the density of the medium surrounding the jets and lobes may change considerably over the large scales considered here. Some GRGs are associated with the dominant member of a galaxy group (as is the case for instance of the FR I GRG NGC 315; Giacintucci et al. 2011), while others have been detected at high redshift in a likely less dense environment. This has been confirmed more quantitatively by Machalski, Chyzy & Jamrozy (2004), in a comparative study of GRGs and normal sized radio galaxies. They concluded that the jet power and the central galaxy density seem to correlate with the size of radio galaxies. All in all, however, the origin and evolution of GRGs remains unclear. In this paper we argue that soft gamma-ray surveys provide a different way to discover and study these intriguing objects and give therefore a new perspective into their nature and origin.

2 THE SAMPLE

The extent of the emission in radio-loud active galactic nucleus (AGN) ranges from less than 100 kpc up to a few Mpc and so a first step to uncover extended radio galaxies is to study the radio morphology of well-defined samples of AGN. In this work we concentrate on two samples of active galaxies selected in the soft gamma-ray band. This waveband provides a very efficient way to find nearby AGN since it is transparent to obscured regions/objects, i.e. those that could be missed at other frequencies such as optical, ultraviolet (UV) and even X-rays. This waveband favours the discovery of 'radiative mode' objects, one of the two main flavours of the AGN radio population (see Heckman & Best 2014 for a review of each population properties). The alternative name for these sources, high ionization or high-excitation AGN, is related to the level of ionization of the narrow-line region gas. In the 'radiative mode' AGN, accretion is postulated to occur via a radiatively efficient accretion disc (e.g. Shakura & Sunyaev 1973). The current soft gamma-ray instrumentation tends to uncover the brightest active galaxies in the sky and hence to favour the discovery of accretion-dominated AGN, also among radio galaxies.

Since 2002, the soft gamma-ray sky is being surveyed by *INTEGRAL*/Imager on Board the Integral Satellite (IBIS) and subsequently by *Swift*/Burst Alert Telescope (BAT) at energies greater than 10 keV; up to now various all sky catalogues have been released, based on the data collected by these two satellites (see e.g. Bird et al. 2010; Baumgartner et al. 2013). These catalogues contain large fractions of active galaxies, i.e. ∼30 per cent among *INTEGRAL*/IBIS and up to 70 per cent among *Swift*/BAT sources. For the purpose of this work we use one sample extracted from *INTEGRAL*/IBIS and one from *Swift*/BAT data; together these two samples provide the most extensive list of soft gamma-ray selected active galaxies known to date. For *INTEGRAL*, we consider the sample of 272 AGN discussed by Malizia et al. (2012) added with four sources that have been discovered or identified with active galaxies afterwards (Landi et al. 2010; Krivonos et al. 2012; Masetti et al. 2013). For *Swift*/BAT we use the 70-month catalogue of Baumgartner et al. (2013) which lists 822 objects associated with AGN or galaxies; in this case we also consider the sample of 65 unknown objects in an attempt to uncover all possible radio galaxies in the BAT sample.

Then we searched for radio counterparts using the NVSS (Condon et al. 1998), the Faint Images of the Radio Sky at Twenty-cm (FIRST; White et al. 1997) and the SUMSS (Mauch et al. 2003). All together we inspected around 1000 images to uncover those sources that are extended (with lobes and jets) on radio maps and therefore display a double lobe morphology typical of radio galaxies. For each radio galaxy we measured the largest angular size (LAS) in arcsec and then calculated the corresponding projected linear size in Mpc at the source redshift assuming the standard cosmological parameters ($H_0 = 71$ km s^{-1} Mpc^{-1}, $\Omega = 0.27$, $\Omega_\Lambda = 0.73$). For all objects located north of declination -40° we used NVSS maps, the accuracy of which is ∼10 arcsec, i.e. 1/4 of the angular resolution. We also complemented such information with images at 1.4 GHz from the FIRST survey whose smaller point spread function or PSF (5 against 45 arcsec of the NVSS) allows better accuracy (of the order of 1.5 arcsec). Nine objects south of $\delta = -40^\circ$ were searched for in the SUMSS survey, and similarly measured. Here the accuracy is worse, ∼20 arcsec, as a result of a wider PSF. For most objects the LAS value obtained in this way is in quite good agreement with literature information. In a few cases there is some discrepancy, mainly arising from artefacts in the image (e.g. 3C 84 and both Centaurus A and Centaurus B) and/or complex radio structure/environment (e.g. 3C 84 and 3C 120); when relevant, notes are reported in Table 2. Considering that our sample spans a broad range of redshifts, from the local Universe (e.g. 3C 84 at $z = 0.017559$) to intermediate distances, such as the case of 3C 309.1 ($z = 0.905$), the uncertainty in the linear size estimate is not constant in our sample. Conversion factors between the angular and linear scale are given in Table 2 and can be used to estimate the uncertainty on each measurement.

All the information gathered has been summarized in Table 2 where for each source, we list redshift, optical class, radio morphology, soft gamma-ray luminosities as measured by *INTEGRAL*/IBIS in the 20–100 keV band and/or *Swift*/BAT in the 14–195 keV band and data on the radio size. In particular we quote the conversion from arcsec to kpc, the radio size (in arcsec and Mpc) as reported in the literature with relative reference and the radio size (in arcsec and Mpc) measured by us in this work. Soft gamma-ray luminosities have been estimated from our own *INTEGRAL*/IBIS spectra (but see also Malizia et al. 2012 for flux values) or have been taken from Baumgartner et al. (2013) for *Swift*/BAT objects.

3 RESULTS

3.1 Sample characteristics

All together we uncovered 64 radio galaxies with a double lobe morphology plus three objects which display a less clear radio

[1] Note that spectral ages are systematically lower than dynamical ages and it is still unclear which best represents a source intrinsic age (Harwood, Hardcastle & Croston 2015, and references therein).

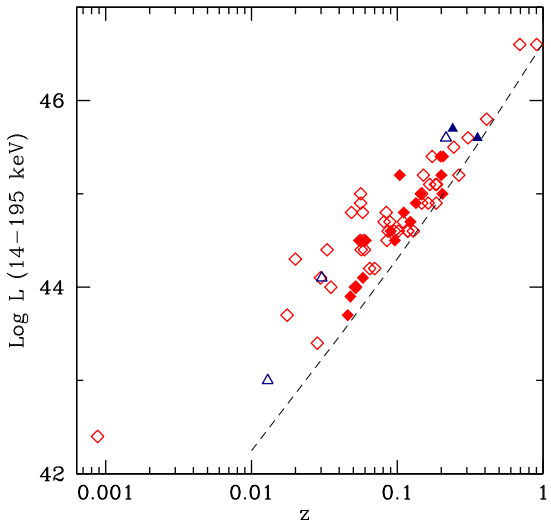

Figure 1. Soft gamma-ray luminosity (14–195 keV) versus redshift for the whole sample. Diamonds are BAT luminosity values while triangles are IBIS ones converted to the proper waveband using a power-law fit to the *INTEGRAL* spectrum; filled symbols represent GRGs. The dashed line represents the sample limiting flux at around 9×10^{-12} erg cm^{-2} s^{-1}.

structure and are therefore candidate radio galaxies. PKS 0921−213 and 2MASX J23272195+1524375 seem to be associated with radio emission made by several components that could belong to a single radio source; the fact that there are no optical objects at the centre of their putative radio lobes is positive but sensitive radio continuum images with lower spatial resolution are necessary to confirm the double lobe morphology of both objects. IGR J18249−3243 is instead unresolved on the NVSS map; it is both the most distant source in the *INTEGRAL*/IBIS complete sample of AGN discussed by Panessa et al. (2015) and the most extended one. Also in this case better imaging is necessary to confirm the double lobe morphology. Interestingly all three candidates have a large radio size, with two objects displaying an extent close to 1 Mpc and this is the main reason why we kept them in the sample although as cases to be confirmed. 27 objects are from the *INTEGRAL* survey, 62 from the *Swift* survey, 22 have a detection in both. The fraction of double lobe radio galaxies which are present in soft gamma-ray catalogues of AGN was found to be around 7 per cent (64/887) for *Swift*/BAT and 10 per cent (27/274) for *INTEGRAL*/IBIS. Only two sources are still optically unclassified: one does not have redshift information while the other has a photometric z value.

Fig. 1 is a plot of the soft gamma-ray (14–195 keV) luminosity versus redshift for the whole sample.[2] As shown in Fig. 1 the sample flux limit is around 9×10^{-12} erg cm^{-2} s^{-1}. The redshift values span from 0.0008 to 0.905 with a mean at 0.136 while the luminosities range from Log ($L_{14-195\,\mathrm{keV}}$) = 42.4 erg s^{-1} to Log($L_{14-195\,\mathrm{keV}}$) = 46.6 erg s^{-1} with a mean at Log($L_{14-195\,\mathrm{keV}}$) = 44.7 erg s^{-1}; these luminosities are quite high, intermediate between Seyfert and blazar values (see for comparison Malizia et al. 2012; Baumgartner et al. 2013).

As summarized in Table 1, the sample contains AGN of various optical classes and, as expected, it is dominated by FR II objects

[2] BAT luminosities have been preferred for this plot as they cover more sources; IBIS 20–100 keV luminosities for five objects not detected by BAT have been converted to 14–195 keV luminosities using best-fitting spectral parameters.

Table 1. Sample classification.

Opt class	Morph type
25 type 1	51 FR II[a]
12 type 1.2–1.5	6 FR I[a]
9 type 1.8–1.9	6 FR I/FR II
19 type 2	1 C
2 unknown	3 unknown

[a]Including also uncertain types.

since high-excitation AGN (both of type I and II) are generally associated with this type of radio morphology (Buttiglione et al. 2010). We point out that the reverse is not true. Using the observed luminosities, the bolometric correction adopted by Mushotzky et al. (2008) for BAT AGN and by Molina et al. (2014) for IBIS AGN[3] and typical black hole masses in the range 10^7–10^9 $M_\odot$, we estimate Eddington ratios ranging from 0.001 up to 0.1, which suggests that all our objects are indeed efficiently accreting, or 'radiative mode' AGN. To confirm this initial indication, we have also checked the literature to find information regarding the excitation mode of the narrow-line region gas in the host galaxy of each source. We find that around 70 per cent of the sources can be defined as high-excitation objects according to various studies in the literature (Schoenmakers et al. 1998; Lewis, Eracleous & Sambruna 2003; Hardcastle, Evans & Croston 2009; Buttiglione et al. 2010; Landt, Cheung & Healey 2010; Winter et al. 2010; Gendre et al. 2013), while the remaining 30 per cent have no data for an unambiguous classification.

3.2 Radio extent of sample objects

Table 2 reports the largest linear size of the radio galaxies in the sample (Section 2). For completeness in column 8 we also report literature values, based on individual studies. The comparison between the two values is shown in Fig. 2. We point out that the values found in the literature are very inhomogeneous, as they refer to interferometric radio observations whose resolution and frequency are very different from the 0.843–1.4 GHz NVSS/FIRST/SUMSS images, hence it is not surprising that we see some differences. Our measurements are affected by some uncertainties, as described in the previous section, but in any case considering the purpose of the present paper, i.e. estimate the fraction of GRGs in our sample, the difference in size is in all cases irrelevant.

Therefore, considering the good match between our sizes and those reported in the literature and the fact that our estimates cover the entire sample, while literature information are lacking for some sources, for the following discussion we will adopt the values reported in the last column of Table 2, i.e. our own measurements, keeping in mind the uncertainties given on the source size and the mismatch found for some sources.

The size distribution of the radio galaxies in the sample shows an almost continuous coverage, from ∼20 kpc (3C 390.1) up to ∼2 Mpc (2MASX J14364961−1613410), with many sources displaying LAS values above few hundred kpc: indeed 60 per cent of the objects in the sample have sizes above 0.4 Mpc. If we consider the classical threshold to define a GRG out of the 67 radio galaxies in this work, we find 16 objects with size ≥0.7 Mpc, i.e. 24 per cent of the total. Even if we keep a more conservative approach and remove all candidate objects, we still find 14 GRGs; this represents 22 per cent of the sample. Taking into account that a couple

[3] $L_{\mathrm{bol}} = 15\,L_{\mathrm{BAT}}$ and $25\,L_{\mathrm{IBIS}}$.

Table 2. Radio galaxies detected by *INTEGRAL*/IBIS and *Swift*/BAT.

Name[†]	z	Opt class	Radio morph	Log $L^{\dagger}_{\rm IBIS}$ (erg s^{-1})	Log $L^{\dagger}_{\rm BAT}$ (erg s^{-1})	Conv fac (kpc arcsec^{-1})	$\rm LAS_{lit}$ (arcsec)	Ref	$\rm Size_{lit}$ (Mpc)	$\rm LAS_{meas}$ (arcsec)	$\rm Size_{meas}$ (Mpc)
PKS 0018−19	0.095579	Sy1.9	FR II	–	44.6	1.784	252.0	1	0.450	280.0	0.499
PKS 0101−649	0.163000	BLQSO	FR II	–	44.9	2.821	210.0	2	0.592	220.0	0.621
3C 033	0.059700	Sy2	FR II	–	44.4	1.161	257.0	3	0.298	260.0	0.302
PKS 0131−36 (NGC 612)[a]	0.029771	Sy2	FR I/II	–	44.1	0.600	852.0	4	0.511	1056.0	0.634
3C 059	0.109720	Sy1.8	FR II	–	44.7	2.015	199.0	1	0.401	200.0	0.403
3C 062	0.147000	Sy2	FR II	–	44.9	2.589	66.0	1	0.171	80.0	0.207
4C +10.08[b]	0.070000	NLRG	FR II	–	44.2	1.345	104.0	5	0.140	160.0	0.215
B3 0309+411B[c]	0.134000	Sy1	FR II	44.9	44.9	2.395	570.0	6	1.365	480.0	1.150
LCF 2001 J0318+684 (2MASX J03181899)	0.090100	Sy1.9	FR II	44.9	44.6	1.692	906.0	7	1.533	900.0	1.523
3C 84 (NGC 1275)[d]	0.017559	Sy1.5	FR I	43.3	43.7	0.360	75.0	8	0.027	900.0	0.324
3C 098	0.030400	Sy2	FR II	43.9	–	0.612	310.0	3	0.190	300.0	0.184
3C 105	0.089000	Sy2	FR II	44.7	44.7	1.673	309.0	1	0.517	370.0	0.619
3C 109	0.305600	Sy1.8	FR II	–	45.6	4.551	97.0	3	0.441	105.0	0.478
3C 111	0.048500	Sy1	FR II	44.7	44.8	0.956	275.0	1	0.263	210.0	0.201
3C 120[e]	0.033010	Sy1	FR I?	44.3	44.4	0.663	840.0	9	0.557	540.0	0.358
PKS 0442−28	0.147000	Sy2	FR II	–	45.0	2.589	86.0	1	0.223	90.0	0.233
Pic A	0.035058	Liner/Sy1	FR II	43.9	44.0	0.702	432.0	1	0.303	420.0	0.295
PKS B0521−365	0.056546	Sy1	FR I/II	44.2	44.4	1.104	60.0	10	0.066	45.0	0.050
PKS 0707−35	0.110800	Sy2	FR II	–	44.8	2.032	486.0	1	0.988	500.0	1.016
3C 184.1	0.118200	Sy2	FR II	–	44.6	2.150	182.0	3	0.391	180.0	0.387
B3 0749+460A	0.051799	Sy1.9	FR II	–	44.0	1.017	120.0	1	0.122	140.0	0.142
3C 206	0.197870	Sy1.2	FR II	–	45.4	3.298	189.0	11	0.623	205.0	0.676
4C +29.30	0.064715	Sy2	FR I/II	–	44.2	1.251	520.0	12	0.650	520.0	0.650
3C 227	0.086272	Sy1.5	FR II	–	44.6	1.627	227.0	1	0.369	230.0	0.374
4C +73.08 (VII Zw 292)	0.058100	Sy2	FR II	–	44.1	1.132	780.0	1	0.883	827.0	0.936
3C 234	0.184925	Sy1.9	FR II	–	44.9	3.125	113.0	1	0.353	115.0	0.359
PKS 1143−696	0.244000	Sey1.2	FR II	45.2	45.5	3.872	–	–	–	150.0	0.581
IGR J13107−5626[f]	–	–	FR II?	− 11.1	− 10.8	–	–	–	–	420.0	–
Centaurus A[g]	0.000880	Sey2	FR I	42.0	42.4	0.018	29520	13	0.531	25200	0.454
Centaurus B	0.012916	NLRG	FR I/II	42.8	–	0.266	1440.0	14	0.383	1600.0	0.426
3C 287.1	0.215600	Sy 1	FR II	45.2	–	3.526	117.0	1	0.413	120.0	0.423
NVSS J143649−161339 (2MASX J14364961)	0.144537	BLQSO	FR I/II	–	45.0	2.553	720.0	15	1.838	714.0	1.823
IGR 14488−4008	0.123000	Sy1.2	FR II	44.3	44.7	2.225	692.0	16	1.540	692.0	1.540
3C 309.1	0.905000	Sy1.5	C	–	46.6	7.910	2.1	1	0.017	2.0	0.016
4C +63.22	0.204000	Sy1	FR II	–	45.0	3.377	210.0	6	0.709	210.0	0.709
3C 323.1	0.264300	Sy1.2	FR II	–	45.2	4.107	70.4	1	0.289	100.0	0.411
4C +23.42	0.118000	Sy1	FR I	–	44.6	2.147	–	–	–	150.0	0.322
S5 1616+85 (Leda 100168)	0.183000	Sy1	FR II	–	45.1	3.099	87.0	1	0.270	140.0	0.434
3C 332	0.151019	Sy1	FR II	–	45.2	2.648	73.0	1	0.193	100.0	0.265
WN 1626+5153 (Mrk 1498)	0.054700	Sy1.9	FR II	–	44.5	1.070	1140.0	5	1.220	1125.0	1.204
4C +34.47	0.206000	Sy1	FR II	–	45.4	3.403	259.0	17	0.881	240.0	0.817
PKS 1737−60	0.410000Phot	–	FR II	–	45.8	5.507	78.0	1	0.430	90.0	0.496
4C +18.51	0.186000	Sy1	FR II	–	45.1	3.140	212.0	1	0.666	220.0	0.691
IGR J17488−2338	0.240000	Sy1.5	FR II	45.2	–	3.825	370.0	18	1.415	370.0	1.415
3C 380	0.692000	Sy1.5	FR II	–	46.6	7.199	7.5	19	0.054	15.0	0.108
3C 382	0.057870	Sy1	FR II	44.5	44.8	1.129	186.0	3	0.210	180.0	0.203
3C 390.3	0.056100	Sy1.5	FR II	44.6	44.9	1.096	229.0	3	0.251	230.0	0.252
PKS 1916−300[g]	0.166819	Sy1.5/1.8	FR II	44.8	45.1	2.875	45.0	20	0.129	150.0	0.431
3C 403	0.059000	Sy2	FR II	44.2	44.5	1.149	97.0	1	0.111	250.0	0.287
Cygnus A	0.056075	Sy1.9	FR II	44.8	45.0	1.095	122.0	21	0.136	115.0	0.126
PKS 2014−55	0.060629	Sy2	FR I	–	44.5	1.178	1284.0	22	1.513	1260.0	1.484
4C +21.55	0.173500	Sy1	FR II	45.1	45.4	2.969	–	–	–	192.0	0.570
4C +74.26	0.104000	Sy1	FR II	45.0	45.2	1.922	610.0	5	1.172	630.0	1.211
S5 2116+81(2MASX J21140128)	0.084000	Sy1	FR I	44.7	44.8	1.589	360.0	6	0.572	340.0	0.540
4C 50.55	0.020000	Sy1	FR II	44.0	44.3	0.408	570.0	23	0.233	468.0	0.191
3C 433	0.101600	Sy2	FR I/II	–	44.6	1.883	69.0	3	0.130	45.0	0.085
PKS 2135−14	0.200470	Sy1.5	FR II	–	45.2	3.332	160.0	1	0.533	150.0	0.500
PKS 2153−69	0.028273	Sy1	FR II	–	43.4	0.571	60.0	24	0.034	80.0	0.046
MG3 J221950+2613 (2MASX J22194971)	0.085000	Sy1	FR II	–	44.5	1.606	–	–	–	200.0	0.321
3C 445	0.055879	Sy1.5	FR II	–	44.5	1.092	570.0	25	0.622	600.0	0.655
3C 452	0.081100	Sy2	FR II	44.6	44.7	1.539	278.0	3	0.428	280.0	0.431
PKS 2300−18	0.128929	Sy1	FR II?	–	44.6	2.317	280	26	0.649	270.0	0.626
PKS 2331−240	0.047700	Sy2	FR II	–	43.9	0.941	1260	27	1.186	1248.0	1.174
PKS 2356−61	0.096306	Sy2	FR II	–	44.5	1.796	410	22	0.736	400.0	0.718

Table 2. – *continued*

Name†	z	Opt class	Radio morph	Log $L^{\ddagger}_{\rm IBIS}$ (erg s^{-1})	Log $L^{\ddagger}_{\rm BAT}$ (erg s^{-1})	Conv fac (kpc arcsec^{-1})	$\rm LAS_{lit}$ (arcsec)	Ref	$\rm Size_{lit}$ (Mpc)	$\rm LAS_{meas}$ (arcsec)	$\rm Size_{meas}$ (Mpc)
				Candidates							
PKS 0921−213	0.052000	Sy1		–	44.0	1.021				1050.0	1.072
IGR J18249−3243	0.355000	Sy1		45.4	–	5.032				100.0	0.503
2MASX J23272195+1524375	0.045717	Sy1		–	43.7	0.904				1020.0	0.922

†We have used the radio source name; the name used in the soft gamma-ray surveys is reported in parenthesis if not coincident with the radio one.
‡IBIS luminosity in the 20–100 keV band. BAT Luminosity in the 14–195 keV band; note that the luminosity of NGC 1275 could be contaminated by the Perseus cluster; similarly is the case of Cen B where the *INTEGRAL* luminosity could be contaminated by the nearby AGN 4U 1344−60.
[a]Our LAS measurement takes into account the northern extension of the western lobe, which explains the difference with the value reported in the literature.
[b]Our LAS measurement takes into account the two tails visible on the NVSS image.
[c]The difference in source size is irrelevant in this case given that both measurements provide a size well above the threshold for GRGs definition.
[d]This radio galaxy is located at the centre of the Perseus cluster and is surrounded by the well-known minihalo (e.g. Bentjens 2011); our measurement refers to the current activity of the AGN.
[e]The morphology of this source is very complex; our measurement refers to the largest extension (in the north–south direction) visible on NVSS.
[f]This source is detected at the reported flux (log F in units of erg cm^{-2} s^{-1}) but we are unable to estimate the luminosity without a knowledge of the source redshift.
[g]For Cen A we have adopted the redshift corresponding to the latest distance estimate of 3.8 Mpc (Harris, Rejkuba & Harris 2010).
[h]The source dimension quoted in the literature for this source comes from a very old radio map while our estimate is based on the NVSS image.
References: 1 – Nilsson (1998); 2 – Sadler et al. (2006); 3 – Leahy, Bridle & Strom in http://www.jb.man.ac.uk/atlas/; 4 – Gopal-Krishna & Wiita (2000); 5 – Landt & Bignall (2008); 6 – Ishwara-Chandra & Saikia (1999); 7 – Lara et al. (2001); 8 – Pedlar et al. (1990); 9 – Walker, Benson & Unwin (1987); 10 – Liuzzo et al. (2013); 11 – Reid, Kronberg & Perley (1999); 12 – Jamrozy et al. (2007); 13 – Eilek (2014); 14 – Jones, Lloyd & McAdam (2001); 15 – Letawe et al. (2004); 16 – Molina et al. (2015); 17 – Hocuk & Barthel (2010); 18 – Molina et (2014); 19 – Nilsson et al. (1993); 20 – Duncan & Sproats (1992); 21 – Carilli, Perley & Harris (1994); 22 – Saripalli & Subrahmanyan (2009); 23 – Molina et al. (2007); 24 – Worrall et al. (2012); 25 – Hardcastle et al. (1998); 26 – Hunstead et al. (1984); 27 – Massardi, Ekers Ronald & Murphy (2008).

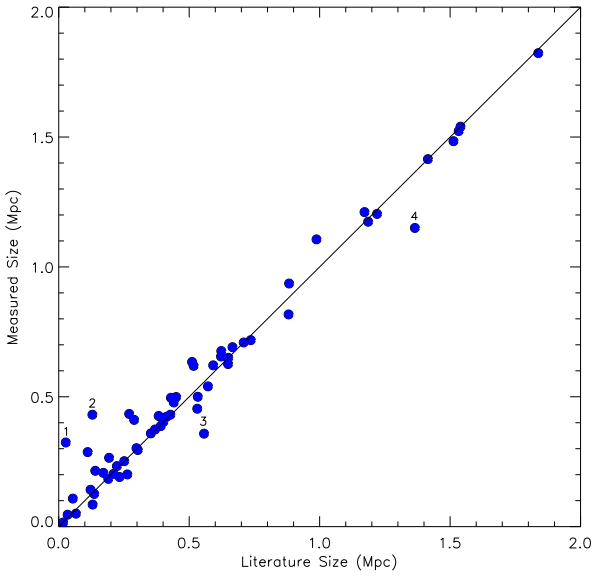

Figure 2. Measured versus literature size both in Mpc. Straight line represents the 1–1 correspondence between sizes. Numbers correspond to some sources with notes in Table 2: 1 = 3C 084/NGC 1275; 2 = PKS 1916−300; 3 = 3C 120; 4 = B3 0309+411B.

of sources (i.e. 3C 206 and 4C +18.51) have dimension close to 0.7 Mpc, this fraction should be considered as a lower limit.

GRGs are very rare objects in the AGN radio-loud population. For instance, in the 3CR catalogue of radio galaxies only 6 per cent are giant (Ishwara-Chandra & Saikia 1999), and if we restrict to the local Universe ($z \leq 0.2$) their fraction decreases to 1 per cent (Andernach et al. 2012). Such small fraction can be interpreted as due to a number of observational biases, which severely affect their inclusion in large samples. The most relevant are the Malmquist bias, which disfavours the detection of faint sources at high redshift, and the linear size bias, which tends to bias high-redshift samples in favour of radio galaxies with very large linear size. i.e. only the peak of the iceberg. At low redshift GRGs are disfavoured both as consequence of the small volume sampled, and of the fact that very diffuse radio lobes may be resolved out by interferometric observations, not to mention that the radio lobes typically have a very steep spectrum, which makes their detection challenging at frequencies above a GHz. Indeed the fraction of GRGs is expected to increase in the new low frequency surveys such as MSSS (Low Frequency Array, LOFAR) and GLEAM (Murchison Widefield Array, MWA). Soft gamma-ray surveys are not affected by these biases, which may explain the considerably higher fraction we report in this paper.

4 PRELIMINARY CONSIDERATIONS

Apart from the selection effects describe above, it is also possible that the difference in the fraction of GRGs found between radio and soft gamma-ray surveys is due to biases related to the sample selection. Our sample is dominated by high-excitation radio galaxies (HERGs) of the FR II type: these are probably among the most powerful objects of the FR II population (Saripalli 2012) and could well be those more capable of producing giant structures. If we consider the sample of FR II radio galaxies discussed by Nilsson (1998), take the radio size of only those objects with redshift and assume the same cosmology adopted in this work, we find that out of 672 objects listed in that work 38 (or 5.6 per cent) qualify to be radio giants. Similarly using the 401 FR II galaxies in the Sloan Digital Sky Survey (SDSS) sample discussed by Koziel-Wierzbowska & Stasinska (2011) we find that 22 objects have size above 0.7 Mpc, i.e. 5.5 per cent of the sample. These percentages are very similar to the one reported for the 3CR sample by Ishwara-Chandra & Saikia (1999). However, both selections do not distinguish between low and high-excitation objects: if this is done for example considering the sample of Buttiglione et al. (2010) where each source is well classified in terms of the relative intensity of low and high-excitation lines, out of 46 high-excitation objects with a reported redshift only one is giant (or 2 per cent of the sample). Thus the radio morphology

of the objects discussed in this work does not seem to provide a bias towards the selection of GRGs.

On the other hand our objects are among the brightest and most powerful AGN in the sky, their soft gamma-ray luminosities are just below those of powerful blazars and their Eddington ratios indicate quite efficient accretors. This immediately suggests that these soft gamma-ray selected radio galaxies have central engines powerful enough to produce large-scale radio structures: a large fraction of the objects in the sample have sizes above few hundred kpc and more than 20 per cent reach giant dimensions. If the soft gamma-ray luminosity is a measure of the source power then one should expect a correlation between this parameter and the source radio size. However no such correlation is evident in the plot of these two quantities shown in Fig. 3.

The analytical models describing the evolution of radio galaxies (see e.g. Kaiser & Alexander 1999 but also Hardcastle & Worrall 2000 and Hardcastle & Krause 2013 for a more realistic approach) indicate that their structure is a function of time, external medium density and jet power; the first and last parameters can be linked to the source central engine. Shabala et al. (2008) find that both the radio source lifetime and duration of the quiescent phase have a strong mass dependence, with massive hosts harbouring longer lived sources that are triggered more frequently.

Indeed in the sample presented in this work, four to five sources (or 25–30 per cent of the sample) display signs of possible restarted activity. PKS 0707−35 shows evidence for a reactivation of the jets accompanied by an axis change (Saripalli, Malarecki & Subrahmanyan 2013); PKS 2014−55, PKS 2356−61, 4C 73.08 and possibly IGR J14488−4008 are X-shaped radio galaxies that display two different lobe alignments as a result of two separate epochs of AGN activity (Saripalli 2007; Saripalli & Subrahmanyan 2009; Molina et al. 2015; Wezgowiec et al. 2016).

On the other hand there is now general consensus that the jet power correlates with the accretion rate and that the most powerful jets are associated with high rates of accretion (Nemmen et al. 2007; Ghisellini et al. 2014). Highly efficient accretion and large black hole mass were indeed found to characterize IGR J14488−4008 and IGR J17488−2338 (Molina et al. 2014, 2015) which are two recently reported GRGs selected in the soft gamma-ray band. This suggests that the most powerful and long living jets, i.e. those capable of producing Mpc radio structures as observed in GRGs, are found in AGN with exceptional internal properties, like large supermassive black holes and high rate of accretion. These are most likely the type of radio galaxies selected by current soft gamma-ray instruments like *INTEGRAL*/IBIS and *Swift*/BAT and collected here for the first time in a large sample. In this case, the lack of a correlation between radio size and soft gamma-ray luminosity (see Fig. 3) may simply reflect the fact that not a single parameter but a combination of parameters provides the condition for the GRGs phenomenon, with the surrounding density medium also playing a role. Indeed Malarecki et al. (2015) show the tendency for radio galaxy lobes to grow to giant sizes in directions that avoid dense regions on both small and large scales, implying that the surrounding environment is an important ingredient in the evolution of giant radio structures.

In order to better understand the reasons that lead to a much higher fraction of GRGs among soft gamma-ray selected AGN, follow up observations of the entire sample are of primary importance; first to define the subsample of GRGs in a better way and then to study the source characteristics (black hole mass, accretion rate, radio ages, detailed radio morphology, environment, etc.) in more details. The analysis of X/soft gamma-ray data of the entire sample has already been performed (Panessa et al. 2016) while the investigation of the radio data is well underway.

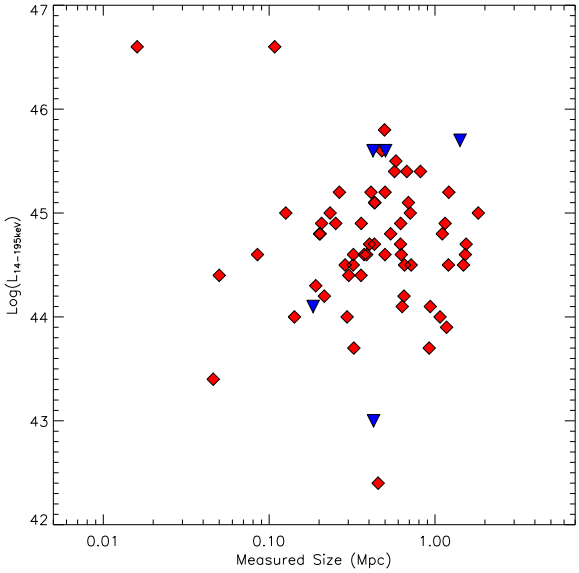

Figure 3. Soft gamma-ray luminosity (14–195 keV) versus measured size; red diamonds are BAT luminosity values while blue triangles are IBIS ones converted to the proper waveband using a power-law fit to the *INTEGRAL* spectrum.

5 SUMMARY

Using recent *INTEGRAL*/IBIS and *Swift*/BAT surveys of AGN we have extracted the first sample of radio galaxies selected in the soft gamma-ray band. The sample consists of 64 objects with a well-defined double lobe morphology plus three candidate sources. The sample covers all optical classes and is dominated by HERG of the FR II type. We have measured the largest angular size of each radio galaxy and found that 60 per cent of the objects in the sample have extensions above 0.4 Mpc and more than 20 per cent has giant radio size ($\geq$0.7 Mpc). We conclude that the fraction of GRGs among soft gamma-ray selected radio galaxies are significantly larger than typically found in radio surveys, where only a few per cent of objects (1–6 per cent) have giant dimensions. This could be due to observational biases affecting the radio but not the soft gamma-ray waveband, thus preventing the detection of GRGs in radio surveys of AGN. On the contrary we do not find any evidence for selection effects due the particular radio morphology/optical type of the objects in the sample. If the soft gamma-ray luminosity is a measure of the source power then one should expect a correlation between this parameter and the source radio size, but this is not evident in the data. This may reflect the fact that more than one parameter is involved in the production of large-scale structure in radio galaxies. Our work indicates that high energy surveys represent a more efficient way to find GRGs than radio surveys.

ACKNOWLEDGEMENTS

We acknowledge the help of four high school students (Nicola Borghi, Enrico Caracciolo, Matteo Rossi and Filippo Cumoli) in the analysis of the radio images; they all participated in a summer school at IASF/INAF Bologna during 2014. This project, being partly conducted by amateur astronomers under the supervision of professional scientists, represents a nice example on how citizen

science work can help in dealing with a large data set. We also acknowledge ASI financial and programmatic support via contracts 2013-025-R0.

REFERENCES

Andernach H., Jiménez Andrade E. F., Maldonado Sánchez R. F., Vásquez Baez I. R., 2012, in Science from the Next Generation Imaging and Spectroscopic Surveys. Published online at http://www.eso.org/sci/meetings/2012/surveys2012/posters.html

Baumgartner W. H., Tueller J., Markwardt C. B., Skinner G. K., Barthelmy S., Mushotzky R. F., Evans P. A., Gehrels N., 2013, ApJS, 207, 19

Bentjens M. A., 2011, A&A, 526, A9

Bird A. J. et al., 2010, ApJS, 186, 1

Blundell K. M., Rawlings S., Willott C. J., 1999, AJ, 117, 677

Buttiglione S., Capetti A., Celotti A., Axon D. J., Chiaberge M., Macchetto F. D., Sparks W. B., 2010, A&A, 509, A6

Carilli C. L., Perley R. A., Harris D. E., 1994, MNRAS, 270, 173

Condon J. J., Cotton W. D., Greisen E. W., Yin Q. F., Perley R. A., Taylor G. B., Broderick J. J., 1998, AJ, 115, 1693

Cotter G., Rawlings S., Saunders R., 1996, MNRAS, 281, 1081

Duncan R. A., Sproats L. N., 1992, Astron. Soc. Aust., Proc., 10, 16

Eilek J. A., 2014, New J. Phys., 16, 5001

Fanaroff B. L., Riley J. M., 1974, MNRAS, 167, 31

Gendre M. A., Best P. N., Wall J. V., Ker L. M., 2013, MNRAS, 430, 3086

Ghisellini G., Tavecchio F., Maraschi L., Celotti A., Sbarrato T., 2014, Nature, 515, 376

Giacintucci S. et al., 2011, ApJ, 732, 95

Gopal-Krishna, Wiita P. J., 2000, A&A, 363, 507

Hardcastle M. J., Krause M. G. H., 2013, MNRAS, 430, 174

Hardcastle M. J., Worrall D. M., 2000, MNRAS, 319, 562

Hardcastle M. J., Alexander P., Pooley G. G., Riley J. M., 1998, MNRAS, 296, 445

Hardcastle M. J., Evans D. A., Croston J. H., 2009, MNRAS, 396, 1929

Harris G. L. H., Rejkuba M., Harris W. E., 2010, Publ. Astron. Soc. Aust., 27, 457

Harwood J. J., Hardcastle M. J., Croston J. H., 2015, MNRAS, 454, 3403

Heckman T. M., Best P. N., 2014, ARA&A, 52, 589

Hocuk S., Barthel P. D., 2010, A&A, 523, A9

Hunstead R. W., Murdoch H. S., Condon J. J., Phillips M. M., 1984, MNRAS, 207, 55

Ishwara-Chandra C. H., Saikia D. J., 1999, MNRAS, 309, 100

Jamrozy M., Konar C., Saikia D. J., Stawarz Ł., Mack K.-H., Siemiginowska A., 2007, MNRAS, 378, 581

Jones P. A., Lloyd B. D., McAdam W. B., 2001, MNRAS, 325, 817

Kaiser C. R., Alexander P., 1999, MNRAS, 302, 515

Koziel-Wierzbowska D., Stasinska G., 2011, MNRAS, 415, 1013

Krivonos R., Tsygankov S., Lutovinov A., Revnivtsev M., Churazov E., Sunyaev R., 2012, A&A, 545, A27

Kronberg P. P., Colgate S. A., Li H., Dufton Q. W., 2004, ApJ, 604, L77

Landi R., Bassani L., Malizia A., Stephen J. B., Bazzano A., Fiocchi M., Bird A. J., 2010, MNRAS, 403, 945

Landt H., Bignall H. E., 2008, MNRAS, 391, 967

Landt H., Cheung C. C., Healey S. E., 2010, MNRAS, 408, 1103

Lara L., Cotton W. D., Feretti L., Giovannini G., Marcaide J. M., Márquez I., Venturi T., 2001, A&A, 370, 409

Lara L., Giovannini G., Cotton W. D., Feretti L., Marcaide J. M., Márquez I., Venturi T., 2004, A&A, 421, 899

Letawe G., Courbin F., Magain P., Hilker M., Jablonka P., Jahnke K., Wisotzki L., 2004, A&A, 424, 455

Lewis K. T., Eracleous M., Sambruna R. M., 2003, ApJ, 593, 115

Liuzzo E. et al., 2013, AJ, 145, 73

Machalski J., Jamrozy M., 2006, A&A, 454, 84

Machalski J., Jamrozy M., Zola S., 2001, A&A, 371, 445

Machalski J., Chyzy K. T., Jamrozy M., 2004, Acta Astron., 54, 249

Malarecki J. M., Staveley-Smith L., Saripalli L., Subrahmanyan R., Jones D. H., Duffy A. R., Rioja M., 2013, MNRAS, 432, 200

Malarecki J. M., Jones D. H., Saripalli L., Staveley-Smith L., Subrahmanyan R., 2015, MNRAS, 449, 955

Malizia A., Bassani L., Bazzano A., Bird A. J., Masetti N., Panessa F., Stephen J. B., Ubertini P., 2012, MNRAS, 426, 1750

Masetti N. et al., 2013, A&A, 556, A120

Massardi M., Ekers Ronald D., Murphy T., 2008, MNRAS, 384, 775

Mauch T., Murphy T., Buttery H. J., Curran J., Hunstead R. W., Piestrzynski B., Robertson J. G., Sadler E. M., 2003, MNRAS, 342, 1117

Molina M. et al., 2007, MNRAS, 382, 937

Molina M., Bassani L., Malizia A., Bird A. J., Bazzano A., Ubertini P., Venturi T., 2014, A&A, 565, A2

Molina M., Venturi T., Malizia A., Bassani L., Dallacasa D., Lal D. V., Bird A. J., Ubertini P., 2015, MNRAS, 451, 2370

Mushotzky R. F., Winter L. M., McIntosh D. H., Tueller J., 2008, ApJ, 684, L65

Nemmen R. S., Bower R. G., Babul A., Storchi-Bergmann T., 2007, MNRAS, 377, 1652

Nilsson K., 1998, A&AS, 132, 31

Nilsson K., Valtonen M. J., Kotilainen J., Jaakkola T., 1993, ApJ, 413, 453

Panessa F. et al., 2015, MNRAS, 447, 1289

Panessa F. et al., 2016, MNRAS, in press

Parma P., Murgia M., Morganti R., Capetti A., de Ruiter H. R., Fanti R., 1999, A&A, 344, 7

Pedlar A. A., Ghataure H. S., Davies R. D., Harrison B. A., Perley R., Crane P. C., Unger S. W., 1990, MNRAS, 246, 477

Reid R. I., Kronberg P. P., Perley R. A., 1999, ApJS, 124, 285

Sadler E. M. et al., 2006, MNRAS, 371, 898

Saripalli L., 2007, From Planets to Dark Energy: the Modern Radio Universe. Published online at SISSA, Proceedings of Science, p. 130

Saripalli L., 2012, AJ, 144, 85

Saripalli L., Subrahmanyan R., 2009, ApJ, 695, 156

Saripalli L., Hunstead R. W., Subrahmanyan R., Boyce E., 2005, AJ, 130, 896

Saripalli L., Malarecki J. M., Subrahmanyan R., 2013, MNRAS, 436, 690

Schoenmakers A. P., Mack K. H., Lara L., Röttgering H. J. A., de Bruyn A. G., van der Laan H., Giovannini G., 1998, A&A, 336, 455

Schoenmakers A. P., de Bruyn A. G., RÖttgering H. J. A., van der Laan H., 2001, A&A, 374, 861

Shabala S. S., Ash S., Alexander P., Riley J. M., 2008, MNRAS, 388, 625

Shakura N. I., Sunyaev R. A., 1973, A&A, 24, 337

Walker R. C., Benson J. M., Unwin S. C., 1987, ApJ, 316, 546

Wezgowiec M., Jamrozy M., Mack K. H., 2016, Acta Astron., 66, 85

White R. L., Becker R. H., Helfand D. J., Gregg M. D., 1997, ApJ, 475, 479

Winter L. M., Lewis K. T., Koss M., Veilleux S., Keeney B., Mushotzky R. F., 2010, ApJ, 710, 503

Worrall D. M., Birkinshaw M., Young A. J., Momtahan K., Fosbury R. A. E., Morganti R., Tadhunter C. N., Verdoes Kleijn G., 2012, MNRAS, 424, 1346

This paper has been typeset from a TEX/LATEX file prepared by the author.